Collective Coordinate Description of Anisotropically Trapped Degenerate Fermi Gases[†]

Seth T. Rittenhouse,*[,‡,||] M. J. Cavagnero,[§] and Chris H. Greene[‡]

Department of Physics and JILA, University of Colorado, Boulder, Colorado 80309-0440 and Department of Physics and Astronomy, University of Kentucky, Lexington, Kentucky 40506-0055

Received: May 31, 2009; Revised Manuscript Received: October 14, 2009

The solution of the many-body Schrödinger equation using an adiabatic treatment of the hyperradius is generalized to treat two components of a hyperspherical vector adiabatically. This treatment has advantages in certain physical situations, such as the description of a degenerate Fermi gas or Bose−Einstein condensate in an anisotropic trapping potential. A first application to the zero-temperature anisotropic Fermi gas is compared with predictions of the Hartree−Fock method.

The many-fermion problem with tunable s-wave interactions continues to generate extensive theoretical and experimental interest. The two-body physics of the Fano-Feshbach resonance is crucial in this system for controlling the s-wave scattering length, a. By using such a resonance, the mean-field interaction strength can be tuned through a wide range of values ranging from attractive ($a < 0$) to repulsive ($a > 0$). It was suggested by Leggett in 1980[1] and later by others[2−4] that this system provides a unique opportunity to study the crossover behavior between Bardeen−Cooper−Schrieffer (BCS) type superfluidity, caused by momentum-correlated pairs of fermions, to a Bose−Einstein condensate (BEC) of diatomic molecules. Interestingly, this connection between two different types of superfluidity is predicted to happen smoothly, without a phase transition. Since these predictions were made long ago, the experimental realization of this crossover has been achieved,[5−10] and theoretical descriptions of the strongly interacting regime abound, from quantum Monte Carlo treatments[11,12] to extensions of the BCS wave function into the unitarity regime of very large magnitude scattering lengths.[13−16]

Most existing theoretical studies of these degenerate Fermi gases (DFGs) explore either a homogeneous gas, which can be related to a harmonically trapped gas through the use of the local density approximation, or else a gas in a spherically symmetric oscillator trap. Although these studies can lead to interesting predictions of phenomena in such a system; experimentally, the gas is often held in an anisotropic cigar-shaped trap.[6−10] With that in mind, in this study we introduce a simple variational treatment of the problem in which the behavior of the gas is described by two collective coordinates that can be thought of as parameterizing the overall longitudinal and transverse spatial extent of the gas.

The starting point for this study is akin to the hyperspherical K-harmonic method presented in refs 17 and 18 in which the DFG was described by a set of $3N - 1$ angular coordinates on the surface of a $3N$ dimensional hypersphere of radius R where N is the total number of particles in the system. To incorporate an anisotropic trap in that formulation would require a very high order in hyperspherical harmonics, and would result in a complex system of coupled 1D differential equations. To avoid these complications here we implement a hypervectorial formulation, which is based on the division of the total $3N$ dimensional space into two physically meaningful subspaces, the set of all transverse coordinates, and the set of all longitudinal coordinates. The division can be thought of as describing the gas by $3N - 2$ angular coordinates on the surface of a $3N$ dimensional hyper-cylinder with height R_z and cylindrical radius R_ρ. These coordinates have been used previously to describe a Bose−Einstein condensate in cigar-shaped and completely anisotropic traps in refs 19 and 20. Their method is extended in this paper to describe the degenerate Fermi gas. While this simple description is not perfect, the goal is to create a simple intuitive picture that reproduces the qualitative meanfield behavior of the system and constitutes an initial step that can be extended in future work.

This paper is arranged as follows; In Section I we introduce the hypervectorial method. In Section II we apply this method to the case of the two-component degenerate Fermi gas with density-dependent, zero-range interactions and analyze the resulting potential surfaces. In Section III we predict the ground state energy and average spatial extent of the system. Section IV uses the potential surface to extract the frequency of low-energy excitations. Section V provides a brief summary and discusses avenues of future inquiry.

I. The Hypervectorial Method

The use of hyperspherical coordinates is well suited to an isotropic oscillator trap because the trapping potential is proportional to the square of the hyperradius.[17,18,21] This is not the case in an anisotropic trap, where different Cartesian coordinates in the trap are associated with different oscillator frequencies. This study will deal with a cylindrically symmetric cigar-shaped trap, but with minor modifications the methods presented here carry over to a completely anisotropic trap. The Hamiltonian for this system is given by

$$H = -\frac{\hbar^2}{2m}\sum_{i=1}^{N}\nabla_i^2 + \frac{1}{2}m\sum_{i=1}^{N}(\omega_\perp^2(x_i^2 + y_i^2) + \omega_z^2 z_i^2) + \sum_{i>j} U_{\mathrm{int}}(r_{ij}) \quad (1)$$

where ω_z and $\omega_\perp$ are oscillator frequencies in the longitudinal and transverse directions, respectively. Here x_i, y_i, and z_i are

[†] Part of the "Vincenzo Aquilanti Festschrift".

* To whom correspondence should be addressed. E-mail: srittenhouse@cfa.harvard.edu.

[‡] University of Colorado.

[§] University of Kentucky.

[||] Current address: ITAMP, Harvard-Smithsonian Center for Astrophysics, Cambridge, MA 02138.

10.1021/jp9051006
Published on Web 11/10/2009

the Cartesian coordinates of the ith atom, and r_{ij} is the interparticle distance between particles i and j.

Now consider two collective coordinates, R_z and R_ρ, given by the rms longitudinal and transverse size of the gas, respectively, that is,

$$R_z^2 = \frac{1}{N}\sum_{i=1}^{N} z_i^2 \tag{2}$$

$$R_\rho^2 = \frac{1}{N}\sum_{i=1}^{N} (x_i^2 + y_i^2) \tag{3}$$

The remaining $3N - 2$ spatial degrees of freedom in the gas are described by angles. The first N angles are merely the cylindrical polar angles for each atom $\{\phi_i\}_{i=1}^{N}$, while the remaining $2N - 2$ angles are given by[22,23]

$$\tan\beta_i = \frac{\sqrt{\sum_{j=1}^{i} z_j^2}}{z_{i+1}} \tag{4}$$

$$\tan\alpha_i = \frac{\sqrt{\sum_{j=1}^{i} (x_j^2 + y_j^2)}}{\rho_{i+1}} \tag{5}$$

where $0 \le \beta_i, \alpha_i \le \pi/2$ and $1 \le i \le N - 1$. The exact parametrization is arbitrary, as these angles will not be used directly, but they are given here for completeness. Collectively these $3N - 2$ hyperangles will be referred to as $\Omega = (\Omega_1, \Omega_2)$ where Ω_1 corresponds to the sub-hyperangles describing the transverse coordinates and Ω_2 the longitudinal sub-hyperangles. The differential volume element $d\Omega$ associated with these coordinates can be extracted using the procedure described in Section Two of ref 23. In these coordinates the sum of the Laplacians in eq 1 can be written in terms of the hypervectorial coordinates as:[22,23]

$$\sum_i^N \nabla_i^2 = \frac{1}{N}\left[\frac{1}{R_\rho^{2N-1}}\frac{\partial}{\partial R_\rho}R_\rho^{2N-1}\frac{\partial}{\partial R_\rho} - \frac{\bar{\Lambda}_\perp^2}{R_\rho^2} + \frac{1}{R_z^{N-1}}\frac{\partial}{\partial R_z}R_z^{N-1}\frac{\partial}{\partial R_z} - \frac{\bar{\Lambda}_z^2}{R_z^2}\right] \tag{6}$$

where $\bar{\Lambda}_\perp^2$ and $\bar{\Lambda}_z^2$ are given by[22]

$$\bar{\Lambda}_z^2 = -\sum_{i>j}\Lambda_{zij}^2$$
$$\bar{\Lambda}_\perp^2 = -\sum_{l>m}\Lambda_{\perp lm}^2$$
$$\Lambda_{zij} = z_i\frac{\partial}{\partial z_j} - z_j\frac{\partial}{\partial z_i}$$
$$\Lambda_{\perp lm} = x_l\frac{\partial}{\partial x_m} - x_m\frac{\partial}{\partial x_l}$$

The sums over i and j (l and m) run over all Cartesian coordinates in the longitudinal (transverse) subspace. Combining eqs 2,3, and 6, the Hamiltonian in eq 1 can be rewritten in terms of the hypervectorial coordinates:

$$H = -\frac{\hbar^2}{2M}\left[\frac{1}{R_\rho^{2N-1}}\frac{\partial}{\partial R_\rho}R_\rho^{2N-1}\frac{\partial}{\partial R_\rho} - \frac{\bar{\Lambda}_\perp^2}{R_\rho^2}\right] + \frac{1}{2}M\omega_\perp^2 R_\rho^2 - \frac{\hbar^2}{2M}\left[\frac{1}{R_z^{N-1}}\frac{\partial}{\partial R_z}R_z^{N-1}\frac{\partial}{\partial R_z} - \frac{\bar{\Lambda}_z^2}{R_z^2}\right] + \frac{1}{2}M\omega_z^2 R_z^2 + \sum_{i>j} U_{\mathrm{int}}(r_{ij}) \tag{7}$$

where $M = Nm$.

The key to the hypervectorial method presented here is similar to the K-harmonic approximation,[17,18] which is based on a variational ansatz wave function,

$$\Psi(R_\rho, R_z, \Omega_1, \Omega_2, \sigma_1, \sigma_2, ..., \sigma_N) = F(R_\rho, R_z)Y_{\lambda_\perp\lambda_z\mu}(\Omega_1, \Omega_2, \sigma_1, \sigma_2, ..., \sigma_N) \tag{8}$$

where $Y_{\lambda_\perp\lambda_z\mu}(\Omega_1, \Omega_2, \sigma_1, \sigma_2, ..., \sigma_N)$ is the lowest allowed hyperangular eigenstate for N noninteracting fermions in an anisotropic harmonic trap. Here $(\sigma_1, \sigma_2, ..., \sigma_N)$ are the spin coordinates. By definition, $Y_{\lambda_\perp\lambda_z\mu}$ satisfies the eigenvalue equations

$$\Lambda_\perp^2 Y_{\lambda_\perp\lambda_z\mu}(\Omega_1, \Omega_2) = \lambda_\perp(\lambda_\perp + 2N - 2)Y_{\lambda_\perp\lambda_z\mu}(\Omega_1, \Omega_2) \tag{9}$$

$$\Lambda_z^2 Y_{\lambda_\perp\lambda_z\mu}(\Omega_1, \Omega_2) = \lambda_z(\lambda_z + N - 2)Y_{\lambda_\perp\lambda_z\mu}(\Omega_1, \Omega_2) \tag{10}$$

The subscript μ enumerates the often quite large number of degenerate states for a given $\lambda_\perp$ and λ_z. It would be convenient if $Y_{\lambda_\perp\lambda_z\mu}(\Omega_1, \Omega_2, \sigma_1, \sigma_2, ..., \sigma_N)$ is merely a product of the two eigenfunctions of $\Lambda_\perp^2$ and Λ_z^2, but this is not the case. The permutational symmetry of the system mixes subhyperspherical harmonics together. Fortunately, examining eq 7 with $U_{\mathrm{int}}(r_{ij}) = 0$, it is clear that the anisotropic oscillator is separable in the hypervectorial coordinates.

In ref 17 it was shown that the lowest hyperspherical harmonic for an isotropically trapped system can be written in terms of a Slater-determinant of independent particle wave functions. Because the noninteracting system is separable in hypervectorial coordinates, the hyperangular behavior of the noninteracting system in an anisotropic trap can be written in the same way, that is,

$$Y_{\lambda_\perp\lambda_z\mu}(\Omega_1, \Omega_2, \sigma_1, \sigma_2, ..., \sigma_N) = \frac{D(\vec{r}_1, \vec{r}_2, ..., \vec{r}_N, \sigma_1, \sigma_2, ..., \sigma_N)}{R_\rho^{(2N-1)/2}G_{0K_\perp}^{\perp}(R_\rho)R_z^{(N-1)/2}G_{0K_z}^{z}(R_z)} \tag{11}$$

Here $D(\vec{r}_1, \vec{r}_2, ..., \vec{r}_N, \sigma_1, \sigma_2, ..., \sigma_N)$ is a ground state Slater-determinant of independent particle states, that is:

$$D(\vec{r}_1, \vec{r}_2, ..., \vec{r}_N, \sigma_1, \sigma_2, ..., \sigma_N) = \sum_P (-1)^p \prod_{i=1}^{N} \psi_i(\vec{r}_i)\langle\sigma_i|m_{s_i}\rangle$$

$$\sqrt{\rho}\psi_i(\vec{r}) = A_{n_{\perp_i} n_{z_i} m_i} \exp(-\rho^2/2\boldsymbol{l}_\perp - z^2/2\boldsymbol{l}_z^2) \times \exp(im_i\phi)\left(\frac{\rho}{\boldsymbol{l}_\perp}\right)^{|m_i|+1/2} L_{n_{\perp_i}}^{|m_i|+1/2}\left(\frac{\rho^2}{\boldsymbol{l}_\perp^2}\right) H_{n_{z_i}}\left(\frac{z}{\boldsymbol{l}_z}\right) \quad (12)$$

where the sum runs over all permutations, P, of the N spatial and spin coordinates, $L_n^\gamma(x)$ is a Laguerre polynomial, $H_n(x)$ is a Hermite polynomial, $\boldsymbol{l}_\perp = (\hbar/m\omega_\perp)^{1/2}$, $\boldsymbol{l}_z = (\hbar/m\omega_z)^{1/2}$, and $A_{n_{\perp_i} n_{z_i} m_i}$ is a normalization constant. In eq 11, $K_\perp = \lambda_\perp + N - 3/2$, $K_z = \lambda_z + N/2 - 3/2$, and $G_{\chi K_\perp}^\perp(R_\rho)$ and $G_{\chi K_z}^z(R_z)$ are the subhyperradial behavior of the noninteracting anisotropically trapped gas given by[17,18,22]

$$R_\rho^{(2N-1)/2} G_{\chi K_\perp}^\perp(R_\rho) = A_{\chi K_\perp}^\perp \exp(-R_\rho^2/2\mathscr{L}_\perp^2)\left(\frac{R_\rho}{\mathscr{L}_\perp}\right)^{K_\perp+1} L_\chi^{K_\perp+1/2}\left(\frac{R_\rho^2}{\mathscr{L}_\perp^2}\right)$$

$$R_z^{(N-1)/2} G_{\chi K_z}^z(R_z) = A_{\chi K_z}^z \exp(-R_z^2/2\mathscr{L}_z^2)\left(\frac{R_z}{\mathscr{L}_z}\right)^{K_z+1} L_\chi^{K_\perp+1/2}\left(\frac{R_\rho^2}{\mathscr{L}_\perp^2}\right)$$

Here, $\mathscr{L}_\perp = \boldsymbol{l}_\perp/(N^{1/2})$, $\mathscr{L}_z = \boldsymbol{l}_z/(N^{1/2})$ and $A_{\chi K_\perp}^\perp$ and $A_{\chi K_z}^z$ are normalization constants. It is interesting to note that, despite appearances, eq 11 is independent of the oscillator lengths $\boldsymbol{l}_\perp$ and $\boldsymbol{l}_z$.

The subhyperangular momentum eigenvalues, $\lambda_\perp$ and λ_z, from eqs 9 and 10 are determined by the number of oscillator quanta in $D(\vec{r}_1, \vec{r}_2, ..., \vec{r}_N, \sigma_1, \sigma_2, ..., \sigma_N)$ in the longitudinal and transverse directions respectively:

$$\lambda_\perp = \sum_{i=1}^{N} (2n_{\perp_i} + |m_i|)$$

$$\lambda_z = \sum_{i=1}^{N} n_{z_i}$$

For this treatment we will only consider nondegenerate, filled energy shells in the large particle number limit, but the treatment can be extended to include finite particle numbers and open energy shells. The nondegenerate ground state is found by filling every state in the noninteracting system up to a Fermi energy, ε_F. In the large N limit, which will be the focus of this paper, the Fermi energy is given in terms of the number of atoms by

$$\varepsilon_f \rightarrow \hbar(3N\omega_\perp^2\omega_z)^{1/3} \quad (13)$$

where it has been assumed that there are enough atoms to occupy many longitudinal and transverse modes, that is, the system is still three-dimensional. The energy of the noninteracting system is given in terms of the hyperangular momentum quantum numbers as

$$E_{NI} = \hbar\omega_\perp(\lambda_\perp + N) + \hbar\omega_z(\lambda_z + N/2)$$

In the large N limit, this becomes

$$E_{NI} \rightarrow \frac{\varepsilon_f^4}{4\hbar^3\omega_\perp^2\omega_z} = \frac{\hbar(3N\omega_\perp^2\omega_z)^{4/3}}{4\omega_\perp^2\omega_z} \quad (14)$$

The hyperangular momentum quantum numbers, $\lambda_\perp$ and λ_z, in the large N limit are given by

$$\lambda_z \rightarrow \frac{\varepsilon_F^4}{12\hbar^4\omega_z^2\omega_\perp^2} = \frac{(3N\omega_\perp^2\omega_z)^{4/3}}{12\omega_\perp^2\omega_z^2} \quad (15)$$

$$\lambda_\perp \rightarrow \frac{\varepsilon_F^4}{6\hbar^4\omega_z\omega_\perp^3} = \frac{(3N\omega_\perp^2\omega_z)^{4/3}}{6\omega_\perp^3\omega_z} \quad (16)$$

To employ the variational principle the hyperangular expectation value of the Hamiltonian given in eq 7 must be taken, leaving an effective Schrödinger equation in the collective coordinates, R_ρ and R_z:

$$ER_z^{(N-1)/2}R_\rho^{(2N-1)/2}F(R_\rho, R_z) = \left[-\frac{\hbar^2}{2M}\left(\frac{\partial^2}{\partial R_\rho^2} - \frac{K_\perp(K_\perp+1)}{2MR_\rho^2}\right) - \frac{\hbar^2}{2M}\left(\frac{\partial^2}{\partial R_z^2} - \frac{K_z(K_z+1)}{2MR_z^2}\right) + \frac{1}{2}M\omega_\perp^2R_\rho^2 + \frac{1}{2}M\omega_\perp^2R_z^2 + \sum_{i>j}\langle Y_{\lambda_\perp\lambda_z\mu}|U_{\text{int}}(r_{ij})|Y_{\lambda_\perp\lambda_z\mu}\rangle\right] \times R_z^{(N-1)/2}R_\rho^{(2N-1)/2}F(R_\rho, R_z) \quad (17)$$

Here, $F(R_\rho, R_z)$ has been multiplied by a factor of $R_z^{(N-1)/2}R_\rho^{(2N-1)/2}$ to remove first derivative terms.

To avoid divergences in the large N limit, it is convenient to rescale the effective Schrödinger equation by noninteracting energy and lengths:

$$E = E_{NI}E'$$

$$R_\rho = \sqrt{\langle R_\rho^2\rangle_{NI}}R'_\rho$$

$$R_z = \sqrt{\langle R_\rho^2\rangle_{NI}}R'_z$$

where E_{NI} is the noninteracting energy, and $\langle R_\rho^2\rangle_{NI}$ is the expectation value of the transverse collective coordinate squared given in the large N limit by

$$\langle R_\rho^2\rangle_{NI} = \frac{\hbar}{M\omega_\perp}\left(\lambda_\perp + N - \frac{1}{2}\right) \rightarrow \frac{(3N\gamma)^{4/3}}{6N\gamma}\boldsymbol{l}_\perp^2 \quad (18)$$

with $\gamma = \omega_z/\omega_\perp$. In the large N limit, with this rescaling, eq 17 becomes

$$0 = \left[-\frac{1}{2m^*}\left(\frac{\partial^2}{\partial R_\rho'^2} + \frac{\partial^2}{\partial R_z'^2}\right) + \frac{V_{\text{eff}}(R'_\rho, R'_z)}{E_{NI}} - \frac{E}{E_{NI}}\right] \times R_z'^{(N-1)/2}R_\rho'^{(2N-1)/2}F(R'_\rho, R'_z) \quad (19)$$

Here $m^* = ME_{NI}\langle R_\rho^2\rangle_{NI}/\hbar^2$, and the effective potential, $V_{\text{eff}}(R'_\rho, R'_z)$, is given by

$$\frac{V_{\text{eff}}(R'_\rho, R'_z)}{E_{NI}} = \frac{1}{3R'^2_\rho} + \frac{1}{3}R'^2_\rho + \frac{1}{12\gamma^2 R'^2_z} + \frac{1}{3}\gamma^2 R'^2_z + \frac{V_{int}(R'_\rho, R'_z)}{E_{NI}}$$

$$\frac{V_{\text{int}}(R'_\rho, R'_z)}{E_{NI}} = \frac{\langle Y_{\lambda_\perp\lambda_z\mu}|\sum_{i>j} U_{\text{int}}(r_{ij})|Y_{\lambda_\perp\lambda_z\mu}\rangle}{E_{NI}} \tag{20}$$

with $\gamma = \omega_z/\omega_\perp$. All that remains is to calculate the hyperangular expectation value of the interaction, after which we will have an effective 2D potential surface describing the motion in (R'_ρ, R'_z).

Interaction Matrix Elements. To find the effective hypervectorial potential, a method for evaluating the interaction matrix element in eq 20 must be developed. The fixed R_ρ and R_z matrix element in eq 20 can be rewritten using δ-functions in R'_ρ and R'_z as

$$V_{\text{int}}(R''_\rho, R''_z) = \int \mathrm{d}\Omega \mathrm{d}R'_\rho \mathrm{d}R'_z \delta(R''_\rho - R'_\rho)\delta(R''_z - R'_z) \times Y^*_{\lambda_\perp\lambda_z\mu}(\Omega)\sum_{i>j} U_{int}(r_{ij}) Y_{\lambda_\perp\lambda_z\mu}(\Omega) \tag{21}$$

A convenient way of expressing the δ-functions in this expression is

$$\delta(R''_\rho - R'_\rho) = \lim_{N\to\infty}\left[A^\perp_{0K_\perp}\left(\frac{\sqrt{N\langle R_\rho^2\rangle_{NI}}R'_\rho}{l_\perp R''_\rho}\right)^{\lambda_\perp+N-1/2} \times \exp\left(-\frac{R'^2_\rho N\langle R_\rho^2\rangle_{NI}}{2l_\perp^2 R''^2_\rho}\right)\right] \tag{22}$$

$$\delta(R''_z - R'_z) = \lim_{N\to\infty}\left[A^z_{0K_z}\left(\frac{\sqrt{N\langle R_z^2\rangle_{NI}}R'_z}{l_\perp R''_z}\right)^{\lambda_z+N/2-1/2} \times \exp\left(-\frac{R'^2_z N\langle R_z^2\rangle_{NI}}{2l_z^2 R''^2_z}\right)\right] \tag{23}$$

Combining eqs 21, 22, and 23 and recalling that the definition of $Y_{\lambda_1\lambda_2\mu}$ from eq 11 is independent of the oscillator lengths gives

$$V_{\text{int}}(R'_\rho, R'_z) = \langle Y_{\lambda_\perp\lambda_z\mu}|\sum_{i>j} U_{\text{int}}(r_{ij})|Y_{\lambda_\perp\lambda_z\mu}\rangle = \langle D_{l_{eff_\perp} l_{eff_z}}|\sum_{i>j} U_{\text{int}}(r_{ij})|D_{l_{eff_\perp} l_{eff_z}}\rangle_{3N} \tag{24}$$

where $D_{l_{\text{eff}_\perp} l_{\text{eff}_z}}(\vec{r}_1, \vec{r}_2, ..., \vec{r}_N, \sigma_1, \sigma_2, ..., \sigma_N)$ is a ground state Slater-determinant wave function of N independent noninteracting fermions in an anisotropic cigar-shaped trap with effective oscillator lengths,

$$l_{\text{eff}_\perp} = R'_\rho l_\perp$$
$$l_{\text{eff}_z} = R'_z\frac{\sqrt{\langle R_\rho^2\rangle_{NI}}}{\sqrt{\langle R_z^2\rangle_{NI}}}l_z \tag{25}$$

Here, $\langle R_z^2\rangle_{NI}$ is the expectation value of the square of the longitudinal collective coordinate:

$$\langle R_z^2\rangle_{NI} = \frac{\hbar}{M\omega_z}\left(\lambda_z + \frac{N}{2} - \frac{1}{2}\right) \to \frac{(3N\gamma)^{4/3}}{12N\gamma^2}l_z^2 \tag{26}$$

The subscript $3N$ in eq 24 indicates that the matrix element is taken over all spatial and spin degrees of freedom.

II. Density-Dependent Interactions

Now that interaction matrix elements can easily be calculated, we specify what interaction this will be applied to. The simplest choice would be that the standard zero-range Fermi-pseudopotential. Unfortunately, the overly singular nature of the δ-function interactions leads to an unphysical collapse of the two-component Fermi gas when the scattering length is sufficiently large and negative.[17] To avoid this we will employ the density-dependent zero-range interactions presented in ref 24 and applied within the K-harmonic approximation in ref 18 in which a zero-range interaction is used whose strength is dependent on the density of the gas.

$$U_{\text{int}}(\vec{r}_{ij}) = \frac{4\pi\hbar^2}{m}\frac{\zeta(k_f(\vec{r}_i)a)}{k_f(\vec{r}_i)}\delta(\vec{r}_{ij}) \tag{27}$$

where a is the two-body s-wave scattering length and the Fermi wavenumber $k_f = k_f(\vec{r}) = (6\pi^2\rho^{(1)}(\vec{r}))^{1/3}$ is defined in terms of the single spin component density, $\rho^{(1)}(\vec{r})$.[25] The effect of the density dependent interaction is to impose the appropriate short-range behavior on clusters of particles in a manner similar to that of ref 26. In other words, if a cluster of particles is very close together with rms radius much less than the scattering length, the effective interaction energy they experience is the same as if the scattering length was infinite. This short-range behavior is extracted in ref 24 by considering a two particle system, but the general method may be extended to a larger number of particles. We approximate the dimensionless renormalized function $\zeta(k_f a)$ from ref 24 with

$$\zeta(k_f a) = A + B\arctan(Ck_f a - D) \tag{28}$$

where

$$A = 0.3949$$
$$B = 1.1375$$
$$C = \frac{1 + \tan^2\left(\frac{A}{B}\right)}{B} = 0.9942$$
$$D = \tan\left(\frac{A}{B}\right) = 0.3618$$

Two of the fitting parameters A and B are found by fitting the asymptotic behavior of $\zeta(k_f a)$ as $k_f a \rightarrow \pm\infty$, which are given in ref 24 by

$$\lim_{k_f a \rightarrow \infty} \zeta(k_f a) = 2.1819$$
$$\lim_{k_f a \rightarrow \infty} \zeta(k_f a) = -1.3919$$

Once A and B are determined, the remaining constants C and D in eq 28 are determined by matching the Fermi pseudopotential in the $|k_f a| \ll 1$ limit,[27,28] that is,

$$\frac{4\pi\hbar^2}{m}\frac{\zeta(k_f a)}{k_f} \rightarrow \frac{4\pi\hbar^2 a}{m} \tag{29}$$

In the large N limit, the interaction matrix element can be rewritten in terms of the density, $\rho^{(1)}_{l_{\mathrm{eff}_\perp} l_{\mathrm{eff}_z}}(\rho, z)$, of a single spin component in the ground state of the effective oscillator.[18,29] This density is given by[30]

$$\rho^{(1)}_{l_{\mathrm{eff}_\perp} l_{\mathrm{eff}_z}}(\vec{r}) = \frac{1}{6\pi^2 \boldsymbol{l}_{\mathrm{eff}_z} \boldsymbol{l}^2_{\mathrm{eff}_\perp}}(2\mu)^{3/2} \times \left(1 - (\boldsymbol{l}_{\mathrm{eff}_z} \boldsymbol{l}^2_{\mathrm{eff}_\perp})^{2/3}\frac{z^2/\boldsymbol{l}^4_{\mathrm{eff}_z} + \rho^2/\boldsymbol{l}^4_{\mathrm{eff}_\perp}}{2\mu}\right)^{3/2} \tag{30}$$

where $\mu = (3N)^{1/3}$ is set by $\rho^{(1)}_{l_{\mathrm{eff}_\perp} l_{\mathrm{eff}_z}}(\vec{r})\, \mathrm{d}^3 r = N/2$.

Evaluating the expectation value in eq 24 with U_{int} given by eq 27 and $k_f(r) = (6\pi^2 \rho^{(1)}_{l_{\mathrm{eff}_\perp} l_{\mathrm{eff}_z}}(\vec{r}))^{1/3}$ gives the effective hypervectorial interaction potential

$$\frac{V_{\mathrm{int}}(R'_\rho, R'_z)}{E_{NI}} = \frac{256}{9\pi^2(\sqrt{2}\gamma R'_z R'^2_\rho)^{2/3}} f\left(\frac{k^0_f a}{(\sqrt{2}\gamma R'_z R'^2_\rho)^{1/3}}\right)$$
$$f(x) = \int_0^1 y^6\sqrt{1-y^2}\,\zeta(xy)\mathrm{d}y \tag{31}$$

One should note that the function $f(x)$ is the same as in the hyperradial effective potential of ref 18. Putting everything together yields a total effective hypervectorial potential,

$$\frac{V_{\mathrm{eff}}(R'_\rho, R'_z)}{E_{NI}} = \frac{1}{3R'^2_\rho} + \frac{1}{3}R'^2_\rho + \frac{1}{12\gamma^2 R'^2_z} + \frac{1}{3}\gamma^2 R'^2_z + \frac{V_{\mathrm{int}}(R'_\rho, R'_z)}{E_{NI}} \tag{32}$$

An example of the effective potential is shown in Figure 1 for a trap ratio $\gamma = 1/3$ and an interaction strength of $k^0_f a = -1$.

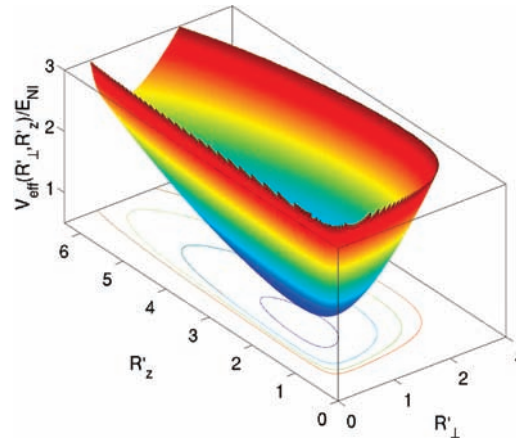

Figure 1. The dimensionless effective hypervectorial potential surface is shown plotted as a function of R'_ρ and R'_z for an interaction strength $k^0_f a = -1$ and a trap ratio of $\gamma = 1/3$.

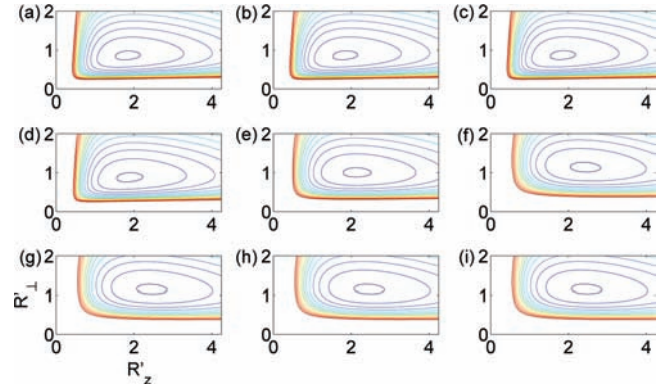

Figure 2. Contour plots of the dimensionless effective hypervectorial potential are shown plotted as a function of R'_ρ and R'_z for an interaction strength varying from $k^0_f a = -12$ to 12 (a−i, respectively) and a trap ratio of $\gamma = 1/3$.

III. Ground State Behavior

Here we analyze the behavior of the effective hypervectorial potential for various values of $k^0_f a$. Figure 2 shows contour plots of V_{eff} for evenly spaced values of $k^0_f a$ from −12 to 12 for a system with trap ratio $\gamma = 1/3$. For attractive interactions ($a < 0$), the minimum is seen to be pulled into the center as the gas pulls in on itself. For repulsive interactions ($a > 0$) the minimum is pushed out away from the center. It is also interesting to see the low lying contours behavior as it gets twisted toward the origin for attractive interactions and away for repulsive. This behavior will be studied in more detail later.

In this section the ground state energy and average squared collective coordinates for the DFG in an anisotropic trap are found, that is, E/E_{NI}, $\langle R'^2_z \rangle$ and $\langle R'^2_\rho \rangle$. Following the same logic as in the hyperspherical K-harmonic method,[18] these quantities can be found by minimizing V_{eff}, that is, by solving $(\partial V_{\mathrm{eff}})/(\partial R'_\rho) = (\partial V_{\mathrm{eff}})/(\partial R'_z) = 0$. The minimum of eq 32 cannot be found analytically, but because the interaction is a function of the product $R'_z R'^2_\rho$ only, the relationship between the minimum longitudinal coordinates, $R'_{z\mathrm{min}}$, and transverse coordinate, $R'_{\rho\mathrm{min}}$, can be found:

$$R'_{z\mathrm{min}} = \frac{R'_{\rho\mathrm{min}}}{\sqrt{2}\gamma} \tag{33}$$

This indicates that, under the assumptions used here, the DFG with density dependent interactions will always maintain the same aspect ratio. This behavior is likely due to the fact that the hyperangular behavior was frozen to the noninteracting behavior. In other words, oscillator quanta cannot be exchanged between the longitudinal and transverse directions, that is, λ_z and $\lambda_\perp$ are fixed. If a more complex formulation were to be used, it is likely that the aspect ratio of the gas would change with repulsive and attractive interactions. For instance, λ_z and

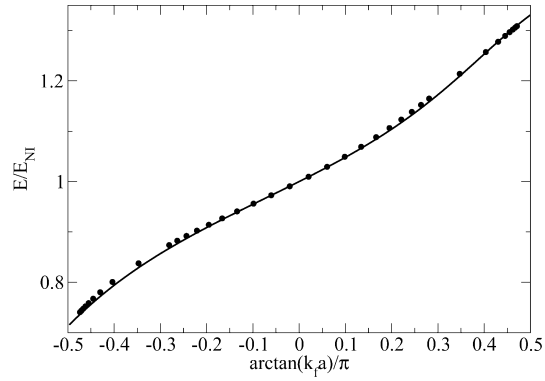

Figure 3. The ground state energy of the DFG in units of the noninteracting energy predicted by the hypervectorial method (solid line) is plotted versus arctan $(k_f^0)/a\pi$ and compared with that predicted by the HF method with 2280 atoms in an isotropic trap (circles).[24]

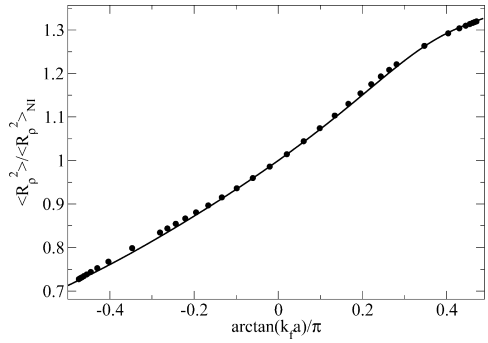

Figure 4. The average squared transverse rms radius of the two-component DFG ground state in the large-N limit, divided by the noninteracting value for this quantity, is plotted vs arctan $(k_f^0)/a\pi$. Also shown are the values predicted by the HF method with 2280 atoms in an isotropic trap (circles).[24]

$\lambda_\perp$ could be considered to be functions of the hypervectorial coordinates $R'_\perp$ and R'_z in the large N limit instead of being fixed by the noninteracting behavior. This extension is beyond the K-harmonic approximation and thus outside the scope of this study.

Inserting eq 33 into eq 32 yields

$$\frac{V_{\text{int}}\left(R'_\rho, R'_z = \frac{R'_\rho}{\sqrt{2}\gamma}\right)}{E_{NI}} = \frac{1}{2R'^2_\rho} + \frac{1}{2}R'^2_\rho + \frac{256}{9\pi^2 R'^2_\rho} f\left(\frac{k_f^0 a}{R'_\rho}\right) \tag{34}$$

This is precisely the same functional form as the effective potential found for the hyperspherical treatment in an isotropic trap, meaning that large N expectation for E/E_{NI} and $\langle R_\rho^2\rangle/\langle R_\rho^2\rangle_{NI}$ in the ground state,shown in Figures 3 and 4, will be exactly the same as E/E_{NI} and $\langle R^2\rangle/\langle R^2\rangle_{NI}$ from ref 18. The average longitudinal rms radius, $\langle R_z^2\rangle/\langle R_\rho^2\rangle_{NI}$ can be extracted using eq 33. Repulsive effective interactions ($a > 0$) should be considered with a grain of salt because the renormalized description of the interactions used here is accurate only if the real two-body interactions are purely repulsive. This means that for this method to be accurate the gas must somehow be prevented from coalescing into molecular dimer states. Further the variational wave function in eq 8 does not incorporate these complex correlations. In other words, with the present initial formulation, we can only consider a gas of atoms, but not of molecules. Figures 3 and 4 also show that the ground state energy and rms radius predicted using the hypervectorial method are in excellent agreement with those predicted using the Hartree−Fock method with the same density-dependent interaction.[24]

IV. Low Energy Excitations

One of the benefits from the hyperspherical K-harmonic approximation of refs 17 and 18 was the simple extraction of the low-lying radial excitations. Similarly, in the hypervectorial picture, low lying excitations can be extracted as well. The difference is that now there are two distinct types of excitation corresponding to transverse and longitudinal breathing modes. In the noninteracting limit these two modes decouple, but as interactions are turned on, excitations in the two trap axes become coupled. This behavior can be visually understood by examining the ellipses made by the low lying contours shown in Figure 2.

A more quantitative view of the low lying excitations can be extracted by normal-mode type of analysis which begins by approximating the effective potential about the minimum as a harmonic oscillator potential,

$$\frac{V_{\text{eff}}(R'_\rho, R'_z)}{E_{NI}} \approx \frac{E_{GS}}{E_{NI}} + \frac{1}{2}[R'_\rho - R'_{\rho\min}, R'_z - R'_{z\min}] \times \begin{bmatrix} \frac{\partial^2 V_{\text{eff}}}{\partial R'^2_\rho} & \frac{\partial^2 V_{\text{eff}}}{\partial R'_\rho \partial R'_z} \\ \frac{\partial^2 V_{\text{eff}}}{\partial R'_\rho \partial R'_z} & \frac{\partial^2 V_{\text{eff}}}{\partial R'^2_z} \end{bmatrix} \begin{bmatrix} R'_\rho - R'_{\rho\min} \\ R'_z - R'_{z\min} \end{bmatrix} \tag{35}$$

where E_{GS} is the ground state energy found by minimizing the effective potential. The oscillator frequencies about this minimum can be extracted by finding the eigenvalues of the Hessian matrix in eq 35

$$\omega_1 = \sqrt{\frac{1}{m^*}\nu_1}$$
$$\omega_2 = \sqrt{\frac{1}{m^*}\nu_2}$$

where ν_1 and ν_2 are the eigenvalues. These breathing modes are in units of the noninteracting energy; to get back to conventional units, the frequencies must be multiplied by $E_{NI}/\hbar$. From eq 19, $m^* = mE_{NI}N\langle R_\rho^2\rangle_{NI}/\hbar^2$, and noting that $N\langle R_\rho^2\rangle_{NI} = 2l_\perp^2 E_{NI}/3\hbar\omega_\perp$ gives

$$\omega_1^B = \sqrt{\frac{3}{2}}\omega_\perp\sqrt{\nu_1}$$
$$\omega_2^B = \sqrt{\frac{3}{2}}\omega_z\sqrt{\nu_2} \tag{36}$$

The eigenvectors corresponding to the eigenvalues in this equation have a direct meaning, as the directions in which the gas oscillates. Roughly, one of these frequencies corresponds to the transverse breathing mode, while the other to longitudinal. We will take ω_1 (ω_2) as the transverse (longitudinal) mode, that is, in the noninteracting limit $\omega_1 = 2\omega_\perp$.

Figures 5 and 6 show the two breathing mode frequencies as a function of $k_f^0 a$ for trap ratios varying from $\gamma = 0.05$ to $\gamma = 0.95$. Again, it should be mentioned that both the variational

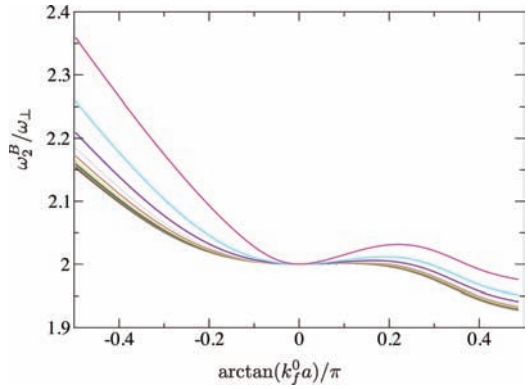

Figure 5. The transverse breathing mode predicted by the hypervectorial method is shown plotted vs the interaction strength $k_f^0 a$ for trap ratios $\gamma = 0.05-0.95$ in steps of 0.1 from bottom to top.

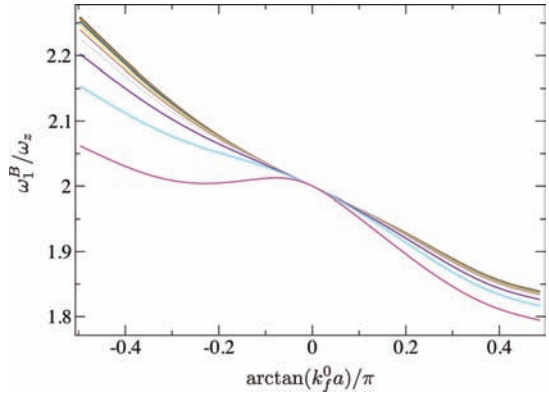

Figure 6. The longitudinal breathing mode predicted by the hypervectorial method is shown plotted vs the interaction strength $k_f^0 a$ for trap ratios $\gamma = 0.05-0.95$ in steps of 0.1 from top to bottom.

trial wave function and the density dependent interaction cannot describe a gas of bosonic dimers for positive scattering lengths. There are several worrying things that can be seen in the predicted behavior of the breathing modes. First, in the unitarity regime, $k_f^0 a \rightarrow -\infty$, both the transverse and longitudinal breathing modes are greater than the noninteracting frequencies for $\gamma < 1$, and the frequencies in this regime depend on γ. This is in disagreement with the unitarity prediction from superfluid hydrodynamic models of $\omega_1^B = (10/3)^{1/2}\omega_\perp$ and $\omega_2^B = (12/5)^{1/2}\omega_z$.[31] Second, and most importantly, the frequencies predicted here differ, both quantitatively and qualitatively, from those found in experiment.[32] These disagreements are likely due to the overly simplistic variational trial wave function, eq 8, used in the hypervectorial picture. By fixing the hyperangular behavior to that of the noninteracting Fermi gas, the wave function cannot take into account the higher order correlations, such as BCS-like pairing, that are present in the system. It should be noted that the K-harmonic method does produce excellent agreement with other predictions[33] for breathing mode frequencies in the unitarity limit for isotropically trapped gases.

V. Summary

In this paper we have presented an extension of the K-harmonic approximation of refs 17 and 18, which incorporates the hypervectorial formulation of ref 19 applied to an anisotropically trapped degenerate Fermi gas. By fixing the subhyperradial coordinates, R_ρ and R_z, a simple 2D effective potential was extracted, allowing for much of the intuition of simple Schrödinger quantum mechanics to be brought to bear on the complex many-body system. The resulting ground state energies were seen to be in perfect agreement with those predicted by the K-harmonic method in an isotropic trap and are in good agreement with those predicted by the Hartree−Fock method. Analysis of the rms spatial extent of the gas showed that, under the hypervectorial approximation presented here, the gas maintains the same aspect ratio throughout the crossover regime. This is likely due to the unphysical assumptions in the distribution of oscillator quanta in the variational wave function, and merits further investigation. Finally, by employing a simple normal-mode analysis, the low energy excitation frequencies of the gas were extracted. While these do not agree with current theoretical predictions[31,34] or experimental results,[32] they do provide an example of the intuitive nature of the method.

While this study does not quantitatively resolve all difficulties, this is seen as a stepping-off point for future studies that hopefully will begin to incorporate the more complex nature of this system. This paper may also be seen as a simple example of the hypervectorial method. While the idea was applied here to a degenerate Fermi gas in an anisotropic trap, this is by no means the only possible application of the technique. For instance, in a Fermi gas of distinguishable particles, for example, a Fermi gas where the components have unequal masses, unequal numbers, or different trapping frequencies, the hypervectorial approach can be applied with each part of the hypervector corresponding to a subhyperradius for each component in the gas. This might allow for higher order fluctuations, phenomena like phase separation, or a "beating" mode where two components oscillate out of phase.

Further applications can be envisioned in the realm of few-body physics. For instance, fixing two total spatial extents in a body-fixed three-body system leaves a simple 1D Schrödinger equation in the remaining degrees of freedom.[35] Similarly, the body-fixed four-body problem can be reduced to a 3D Schrödinger equation,[36] the solution to which can then be carried out using current computation methods.

Acknowledgment. The authors would like to thank Javier von Stecher for providing Hartree−Fock calculations and numerous useful discussions. This work was supported by funding from the NSF.

References and Notes

(1) Leggett, A. J. *J. Phys. C (Paris)* **1980**, *41*, 7.
(2) Nozieres, P.; Schmitt-Rink, S. *J. Low-Temp. Phys.* **1985**, *59*, 195–211.
(3) Drechsler, M.; Zwerger, W. *Ann. Phys. (Germany)* **1992**, *1*, 15–23.
(4) Holland, M.; Kokkelmans, S. J. J. M. F.; Chiofalo, M. L.; Walser, R. *Phys. Rev. Lett.* **2001**, *87*, 120406.
(5) DeMarco, B.; Jin, D. S. *Science* **1999**, *285*, 1703.
(6) Regal, C. A.; Greiner, M.; Jin, D. S. *Phys. Rev. Lett.* **2004**, *92*, 40403.
(7) Kinast, J.; Hemmer, S.; Gehm, M.; Turlapov, A.; Thomas, J. *Phys. Rev. Lett.* **2004**, *92*, 150402.
(8) Zwierlein, M.; Stan, C.; Schunck, C.; Raupach, S.; Kerman, A.; Ketterle, W. *Phys. Rev. Lett.* **2004**, *92*, 120403.
(9) Bartenstein, M.; Altmeyer, A.; Riedl, S.; Jochim, S.; Chin, C.; Denschlag, J.; Grimm, R. *Phys. Rev. Lett.* **2004**, *92*, 120401.
(10) Bourdel, T.; Khaykovich, L.; Cubizolles, J.; Zhang, J.; Chevy, F.; Teichmann, M.; Tarruell, L.; Kokkelmans, S.; Salomon, C. *Phys. Rev. Lett.* **2004**, *93*, 50401.
(11) Astrakharchik, G. E.; Boronat, J.; Casulleras, J.; Giorgini, S. *Phys. Rev. Lett.* **2004**, *93*, 200404.
(12) Chang, S. Y.; Pandharipande, V. R.; Carlson, J.; Schmidt, K. E. *Phys. Rev. A* **2004**, *70*, 43602.
(13) Bulgac, A.; Drut, J. E.; Magierski, P. *Phys. Rev. Lett.* **2006**, *96*, 090404.
(14) Perali, A.; Pieri, P.; Strinati, G. C. *Phys. Rev. Lett.* **2004**, *93*, 100404.
(15) Perali, A.; Pieri, P.; Strinati, G. C. *Phys. Rev. Lett.* **2004**, *93*, 100404.

(16) Tan, S.; Levin, K. *Phys. Rev. A* **2006**, *74*, 43606.
(17) Rittenhouse, S. T.; Cavagnero, M. J.; von Stecher, J.; Greene, C. H. *Phys. Rev. A* **2006**, *74*, 053624.
(18) Rittenhouse, S. T.; Greene, C. H. *J. Phys. B* **2008**, *41*, 205302.
(19) Kim, Y. E.; Zubarev, A. *J. Phys. B* **2000**, *33*, 55.
(20) Kushibe, D.; Mutou, M.; Morishita, T.; Watanabe, S.; Matsuzawa, M. *Phys. Rev. A* **2004**, *70*, 63617.
(21) Bohn, J. L.; Esry, B. D.; Greene, C. H. *Phys. Rev. A* **1998**, *58*, 584.
(22) Avery, J. *Hyperspherical Harmonics: Applications in Quantum Theory*; Kluwer Academic Publishers: Norwell, MA, 1989.
(23) Smirnov, Y. F.; Shitikova, K. V. *Sov. J. Part. Nucl.* **1977**, *8*, 44.
(24) von Stecher, J.; Greene, C. H. *Phys. Rev. A* **2007**, *75*, 022716.
(25) This interaction is appropriate when the Fermi surfaces of two components coincide. When this is not the case, for instance when there is a population imbalance, the different components have different masses or trap frequencies, or in the case of multi-component gases, the interaction must be averaged over the different components.
(26) Tan, S. *arXiv.org* **2004**, DOI: cond-mat/0412764.
(27) Fermi, E. *Ric. Sci.* **1936**, *7*, 13.
(28) Roth, R.; Feldmeier, H. *Phys. Rev. A* **2001**, *64*, 43603.
(29) Cowan, R. D. *The Theory of Atomic Structure and Spectra*; University of California Press: Los Angeles, CA, 1981.
(30) Brack, M.; Bhaduri, R. K. *Semiclassical Physics*; Addison-Wesley: Reading, MA, 1997.
(31) Stringari, S. *Europhys. Lett.* **2004**, *65*, 749–752.
(32) Bartenstein, M.; Altmeyer, A.; Riedl, S.; Jochim, S.; Chin, C.; Denschlag, J. H.; Grimm, R. *Phys. Rev. Lett.* **2004**, *92*, 203201.
(33) Werner, F.; Castin, Y. *Phys. Rev. A* **2006**, *74*, 53604.
(34) Astrakharchik, G. E.; Combescot, R.; Leyronas, X.; Stringari, S. *Phys. Rev. Lett.* **2005**, *95*, 030404.
(35) Littlejohn, R.; Mitchell, K.; Aquilanti, V.; Cavalli, S. *Phys. Rev. A* **1998**, *58*, 3705–3717.
(36) Aquilanti, V.; Cavalli, S. *J. Chem. Soc., Faraday Trans.* **1997**, *93*, 801–809.

JP9051006